BADIÂ AIT EL HAJ[1*], ABOUBAKR BOUAYAD[1], MOHAMMED ALAMI[1]

EFFECT OF TITANIUM ADDITION ON THE PRO-EUTECTIC AND EUTECTIC PHASES OF AlSi9 CAST ALLOY

In this study, the effects of grain size refiner addition and various pre-heating mold temperatures on AlSi9 cast alloy microstructure and solidification have been evaluated. For different process conditions, thermal analysis was performed for all samples and cooling curves were established. Important parameters in liquidus and eutectic Si-phase regions have been calculated using the first derivative cooling curves. Secondary Dendrite Arm Spacing (SDAS) variation was also determined. Experimental results question the effectiveness of cooling curve parameters in providing the microstructure data as a function of refinement. The present work shows that the effect of grain refiner addition on the value of SDAS was higher when the solidification time was lower. It indicated that the solidification parameters such as nucleation temperatures of α-Al phase, undercooling temperature and total solidification time were affected by grain refinement. It has been found that the addition of grain refiner affect the eutectic phase formation time. However, it has no effect on the eutectic phase morphology.

Keywords: AlSi9 cast alloy, grain refinement, thermal analysis, eutectic phase, Secondary Dendrite Arm Spacing (SDAS)

1. Introduction

In the industry, great interest is given to lightweight metals due to their low costs production, ease of machining and good recycling possibilities. Aluminum-silicon alloys (Al-Si) offer good advantage for automotive, aerospace and engineering applications as good castability properties, high corrosion resistance and good physical and mechanical properties [1-5].

During the solidification process, the microstructure determines the final properties of castings. The grain refinement in aluminum alloys is simulated by introducing new nuclei on the primary particles in order to improve the quality of the casting [6]. In casting process, refinement is carried out through three methods: *i – thermal method: cooling rate control; ii – chemical method: grain size refiner addition; iii – mechanical method: agitation of melt during solidification* [7-9].

Over the past years, many researchers have thoroughly studied the effect of grain refinement on microstructure of aluminum alloys. In hypoeutectic aluminum-silicon alloy casting, the particles added in very small amounts of master alloys of Al-Ti, Al-Ti-B or Al-Ti-C to the melt before casting promote refinement. It is generally agreed that when master alloys are added, different intermetallic particles (TiAl3, TiB2, (Al,Ti)B2, TiC or AlB2) are released into the melt to subsequently

act as nucleants [10-13]. The addition of grain refiner induces the creation of heterogeneous nucleation sites which are dispersed in the metal liquid and thus lead to the reduction of the grain size. Therefore, it is necessary to create a large number of solidification nuclei that allow refinement of the structure and that consequently improve the mechanical characteristics [14,15]. Cooling rate is one of the most important variables which determine microstructure and mechanical properties of castings. Increasing the cooling rate reduces the solidification time, refines the grain size and forms dendrites with small size. Solidification time directly affects the ability of the liquid metal to feed the solidifying interdendritic region.

The best technique to assess the degree of grain refinement is the direct measurement from metallographically prepared samples. Although, optical microscopy takes time in preparing samples and requires the cutting of the casting, a chemical analysis determines the amount of grain refiner in the melt but it does not inform about the cooling rate. The thermal analysis of melts as in-situ technique is nowadays extensively used in industry as primary control tool [16,17].

Actually, the cooling curve and/or its derivatives are used to assess the effect of melt treatment on solidification parameters that are correlated to microstructural changes in Al-Si alloys. It is used to estimate alloy composition, grain size, secondary

[1] MOULAY ISMAÏL UNIVERSITY (UMI), ECOLE NATIONALE SUPÉRIEURE D'ARTS ET MÉTIERS (ENSAM), LABORATOIRE DES SCIENCES ET MÉTIERS DE L'INGÉNIEUR, BP 15290 EL MANSOUR, MEKNES, MOROCCO

* Corresponding Author: aitelhaj.badia@gmail.com

dendrite arm spacing (SDAS), solidification latent heat and solid fraction [18-21].Most research on Al-Si alloys has focused on the effect of grain refiners on the characteristic features of the primary Al dendrite and/or the effect of modifiers on the eutectic structure under different solidification conditions. However, to our knowledge, little works has been conducted on the influence of grain refiners on the eutectic features. The aim of this work is to investigate the effects of grain refiner addition and initial mold temperature on the microstructure of AlSi9 alloy. Characteristic features including cooling rate, α-Al dendrite growth temperature, recalescence undercooling, aluminum-silicon eutectic nucleation temperature, aluminum-silicon eutectic growth temperature, solidification time as well as other events related to the solidification were analyzed.

Experimental data obtained using cooling curve thermal analysis (CCTA) were correlated to metallographic analysis. The microstructural feature that has been evaluated is the secondary dendrite arm spacing [22,23].

2. Material and methods

In this study we used an aluminum-silicon alloy EN AC-44400. The latter was melted in silicon carbide crucibles using an electric resistance furnace and maintained at a temperature of 730°C. In order to ensure better control of the pouring temperature, a direct reading of the temperature in the mold was taken by means of type-K thermocouple. The metallic mold used for the cooling curve thermal analysis in this work, named Tatur, is shown in Fig. 1.

The process variable considered in this study is the metallic mold preheat temperature. The mold was coated with lubricant spray (Dycote F39) and preheated at two temperatures 150°C and
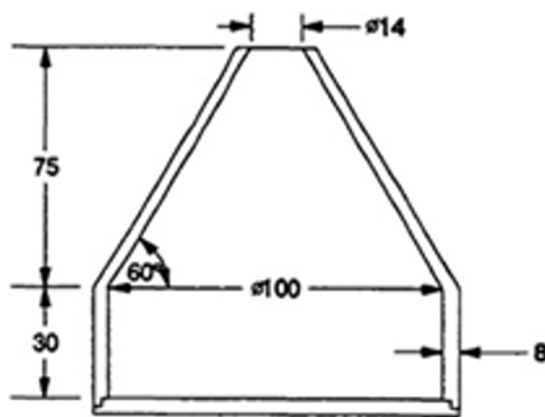

Fig. 1. Permanent mold used to cast TATUR specimen (Dimensions are in mm) [24]

300°C. The initial temperature of the steel mold was measured using contact type thermocouple. Grain refinement can be attained by increasing the cooling rate of casting or grain refiner addition. Titanium based grain refiner was introduced in the melt in the form of potassium fluotitanate (K_2TiF_6) salt. The chemical composition of the untreated and treated alloy corresponds to the average values of three measurements in the sample obtained by a spark emission spectrometer, is shown in Table 1.

The variation of temperature during the solidification process is measured by positioning a thermocouple in the mold cavity receiving molten metal before pouring. Indeed, in order to quantify the temperature change high sensitive K-type thermocouple, protected by a stainless steel sheath, were located in the mold cavity and connected to data acquisition and recording system, as indicated in Fig. 2.

The signal was recorded every 0.5 s for all experiments. The cooling curves (temperature-time curves) were drawn

TABLE 1

Chemical composition of the casting alloy EN AC-44400 (wt.%)

Alloy	ISO Designation	Si	Mg	Fe	Cu	Zn	Mn	Ti	Al
Standard EN AC-44400	AlSi9	8.0-11.0	0.1	0.65 (0.55)	0.1 (0.08)	0.15	0.5	0.15	bal.
Measured		8.626	0.022	0.398	0.064	0.41	0.173	0.013	bal.
Grain-refined sample		8.652	0.015	0.406	0.058	0.414	0.168	0.045	bal.

Fig. 2. Thermal analysis configuration with metallic mold and a thermocouple

by means of dedicated software. Characteristic features including temperature and time related to the start and end of phase transformation, undercooling as well as other events related to the solidification by using CCTA technique were determined.

The analysis of the cooling curves was accompanied by micrographic analysis. The thermal analysis samples were sectioned horizontally through the place that tip of the thermocouple was located, and were ground, polished to 1 μm and etched by Keller's reagent to facilitate observations made under optical microscope (Olympus BX60). The average of more than 10 measurements of the secondary dendrite arm spacing was performed using image analysis software [4]. To calculate the SDAS, the length of the line measured was divided to the number of secondary dendrites arm spacing. SDAS variation depending on refinement and solidification time was evaluated [25].

3. Results and discussion

3.1. Microstructural analysis

SDAS is a microstructural parameter widely used to measure the coarseness of the microstructure in hypoeutectic aluminum-silicon alloys [26]. The secondary dendrite length was determined as the average value of the maximum secondary dendrite lengths in 10 optical fields randomly selected [4].

The changes in SDAS depend on chemical composition, liquid metal treatment, cooling rate/ solidification time and temperature gradient [22].

Microstructures of some samples are shown in Fig. 3. It shows that the dendrite distribution tends to be more homogeneous as the initial mold temperature increases. Fig. 3d) illustrates the combined effect of higher mold temperature and refinement addition on the alloy microstructure. In this case, the formation of fine microstructure and homogeneous distribution of the dendrites has been observed due to uniform distribution of nuclei. In addition, one can notice that adding grain refiner affects the morphology of the dendritic cells that become more spherical (equiaxed structure).

The result of average SDAS measurements in function of the grain refiner addition and mold temperature is shown in Fig. 4. It was found that the untreated sample poured in mold preheated at 300°C has the coarsest primary α-Al phase homogeneously distributed within the metal matrix. The decrease of the initial mold temperature from 300°C to 150°C reduces respectively average SDAS values from 52 μm to 45 μm and from 43 μm to 29 μm for untreated sample and grain refined sample. Consequently, the effect of grain refiner addition when the mold temperature is at 300°C on SDAS is approximately similar to the effect of the initial mold temperature reduction. This confirms that the change of the cooling rate affects the SDAS value. These results are in line with literature for other Al-Si alloys [27]. Decreasing the energetic barrier encourages
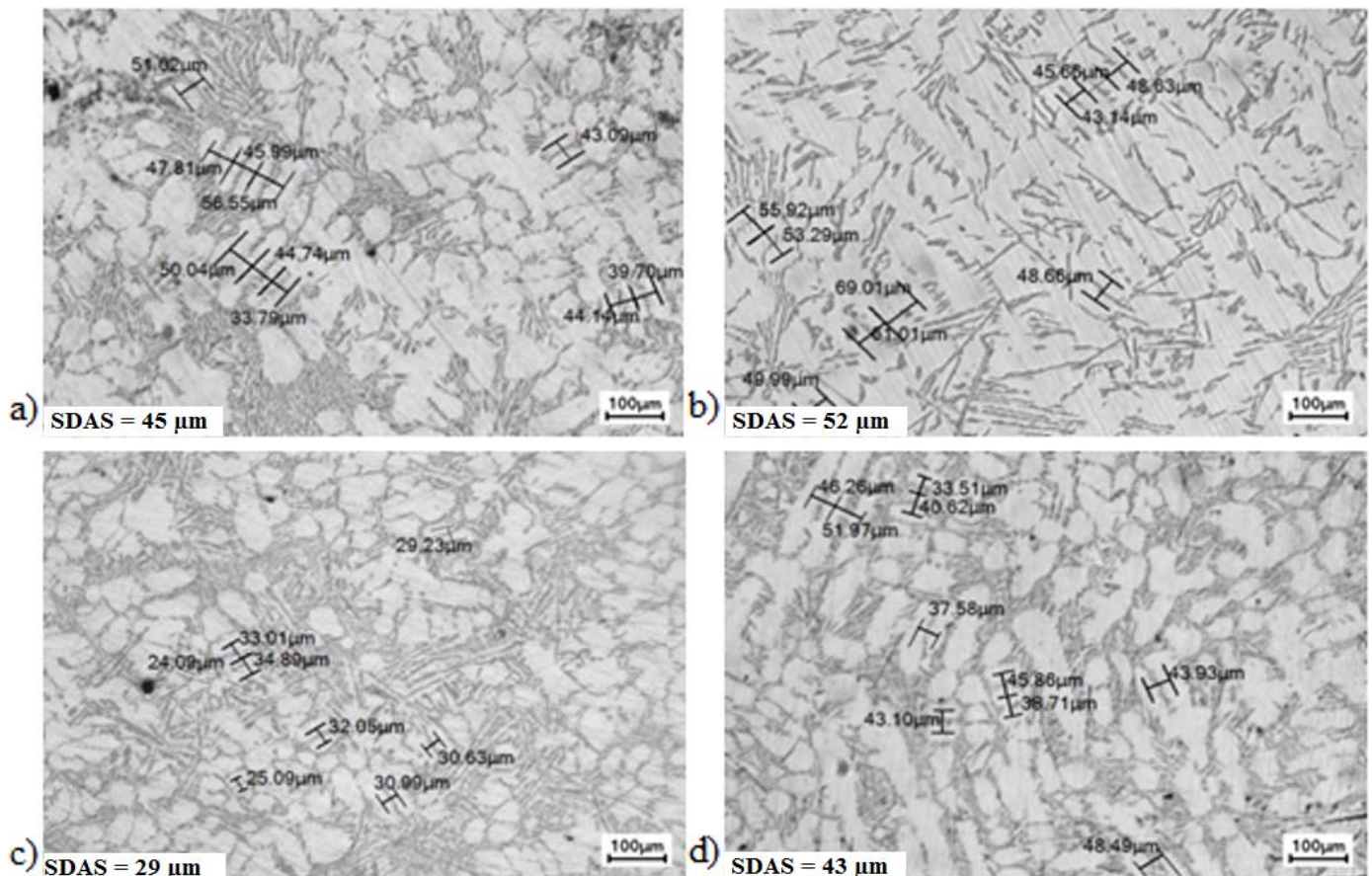

Fig. 3. SDAS measurements in untreated sample at a) $T_{mold} = 150°C$, b) $T_{mold} = 300°C$, grain-refined sample at c) $T_{mold} = 150°C$, d) $T_{mold} = 300°C$
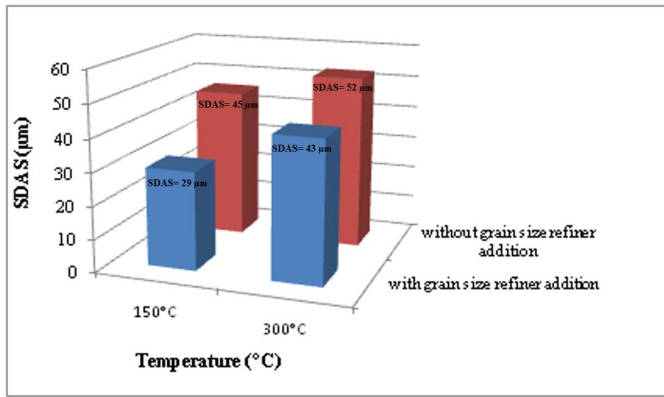
Fig. 4. Variation of SDAS parameter as a function of the grain refiner addition and initial mold temperature

the multiplication of nuclei sites by acting on either cooling rate or adding grain refiner.

Based on the equilibrium phase diagram, dendritic aluminum phase develops prior to the eutectic formation. It is usually believed that the eutectic phase in Al-Si alloy is an interdendritic phase. It is obvious that the hypoeutectic Al-Si alloys properties strongly depend on the size, morphology and distribution of the eutectic silicon. Indeed, to our knowledge, the direct effect of the addition of the grain refiners on the eutectic has not been found. After refiner addition, the SDAS is smaller and consequently the eutectic phase is getting more divided as shown in Fig. 5. However, one can affirm that it has no effect on eutectic phase morphology (acicular).

3.2. Thermal analysis

The refinement level can be determined using both metallographic and thermal analysis techniques. The cooling curves recorded for the AlSi9 cast alloy for different process conditions were used to determine solidification parameters such as liquidus and solidus temperatures and time related to the start and end of phase transformation, cooling rate, undercooling and solidification time. The latter is defined as the time interval elapsed between the liquidus and solidus temperature. The liquidus is related to the nucleation of α-Al primary phase and the solidus is related to the end of solidification. These temperatures and more detailed information pertaining to the alloy's thermal characteristics such as aluminum-silicon eutectic growth temperature, and eutectic time were collected from the first derivative of the cooling curve.

In literature, a noticeable disagreement has been noticed in some solidification parameters determination. In this paper, the average cooling rate has been calculated as the ratio of the temperature difference between liquidus and solidus temperatures to the total solidification time as shown in the following equation:

$$Cooling\ rate = \frac{T_N - T_S}{t_N - t_S} \qquad (1)$$

Where T_N and T_s are liquidus and solidus temperature respectively, t_N and t_s are the time recorded at the beginning and the end of solidification respectively. The other solidification parameters are determined from cooling curves according to the method indicated by Shabestari & Malekan [17] as shown in Fig. 6 and Table 2.

TABLE 2

Solidification characteristic parameters shown in Fig. 6

| Characteristic symbol	Characteristic description
$T_{N,\alpha}$	α-Al dendrite nucleation (liquidus) temperature
T_S	Solidus temperature (end of solidification process)
ΔT_S	Solidification range ($\Delta T_S = T_{N,\alpha} - T_S$)
t_f	Total solidification time
CR_L	Cooling rate in liquidus region
CR	Cooling rate in mushy zone
$T_{Min,\alpha}$	α-Al dendrite minimum temperature
$t_{N,\alpha}$	Nucleation undercooling time
$T_{G,\alpha}$	α-Al dendrite growth temperature
$T_{N,Si}$	Si eutectic nucleation temperature
$T_{G,Si}$	Si eutectic growth temperature
$T_{N,Cu}$	Cu-rich eutectic nucleation temperature
$T_{G,Cu}$	Cu-rich eutectic growth temperature
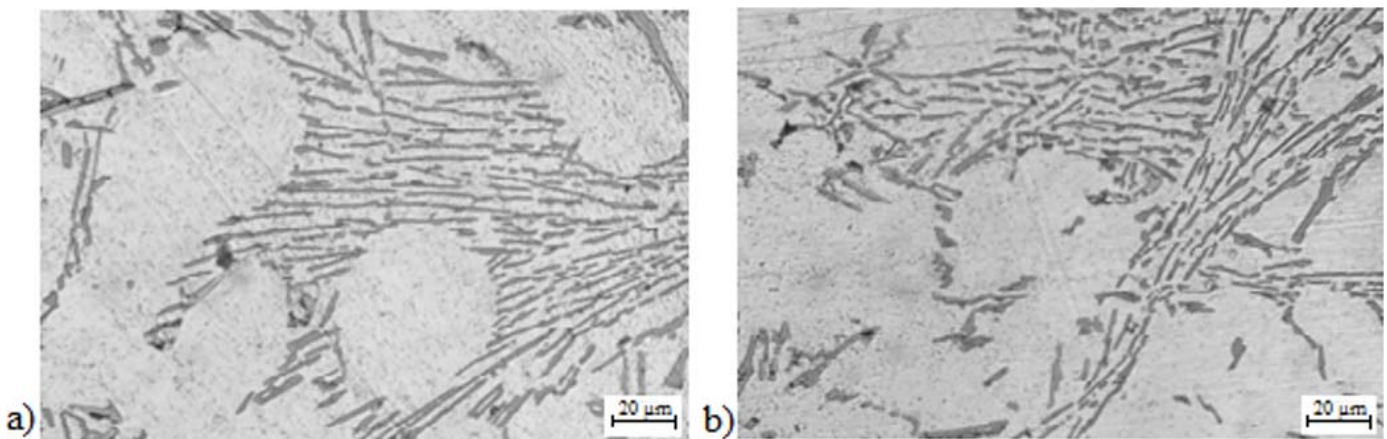
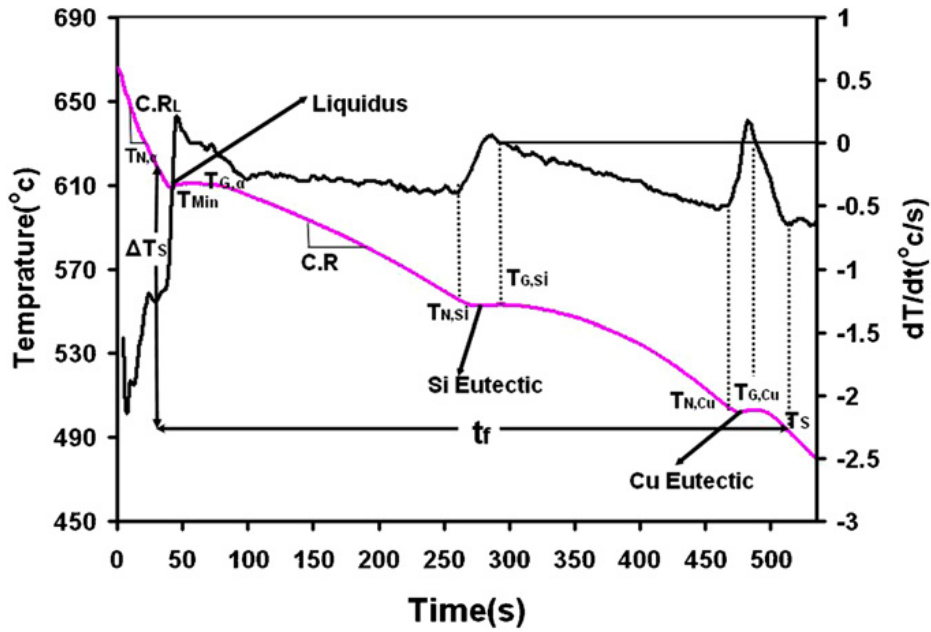Fig. 5. Eutectic area in the a) untreated sample b) grain-refined sample

Fig. 6. Cooling curve, first derivative curve and representation of characteristic parameters for an aluminum alloy [17]

Based on thermal analysis data, the cooling rates were calculated from the cooling curves as 0.1 and 0.25 °C.s⁻¹ corresponding to the mold preheat temperature, of 300 and 150°C respectively. The cooling curves were plotted for each alloy condition.

The Fig. 7 shows the variation of temperature versus time $T = f(t)$ and their derivatives $dT/dt = f'(t)$. During solidification of the AlSi9 alloy, we identified the solidification reactions by curve inflexions. The peaks are corresponding to nucleation and growth of aluminum α-Al dendrite and Al-Si eutectic phases. The

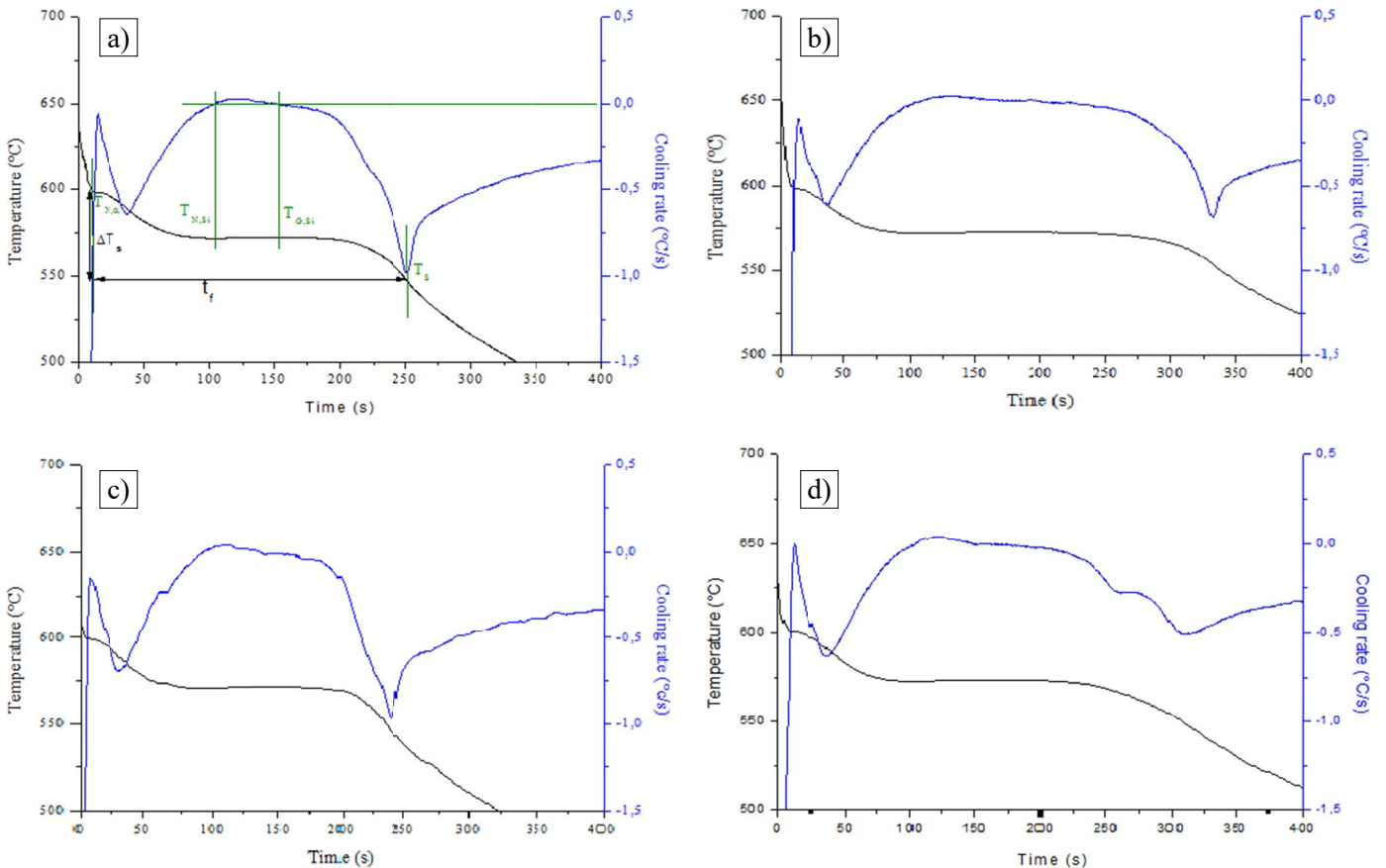Fig. 7. Cooling curves and first derivatives for: a) $T_{mold} = 150°C$ untreated sample, b) $T_{mold} = 300°C$ untreated sample, c) $T_{mold} = 150°C$ grain-refined sample, d) $T_{mold} = 300°C$ grain-refined sample

solidification interval is defined as the temperature difference between the first and the last nuclei liquid to solidify. According to the classical germination theory, the critical nucleation radius is inversely proportional to undercooling and decreasing Gibbs energy barrier. Increasing the undercooling can be beneficial to the reduction of the critical germination radius. As a result, SDAS decreases with decreasing mold temperature due to the multiplication of nucleation sites.

Thermal analysis revealed that the solidification process of the AlSi9 alloy started at 596.1°C and ended at 553.9°C. In the presence of the grain refiner, liquidus temperature raised to 600.5°C, as consequence of α-Al phase nucleation promotion. This is likely due to the increase in the number of nucleation sites. In literature, the increase in nucleation temperature is often associated with a decrease in grain size [28,29].

In comparison, when the mold is preheated to 300°C, the liquidus temperature increases from 598.3°C to 599.4°C after grain refiner addition revealing the effect of the refinement.

The structure of the alloy is strongly related to the number of germination sites present in the liquid metal when the metal reaches liquidus temperature. When the grain refiner is added to the liquid metal, the liquidus temperature increases showing the decrease of the energy barrier. Consequently, we can use liquidus parameters to predict the efficiency of grain refinement treatment. When a percentage of Titanium is added, the solidification interval increases as the solidification time decreases. Fig. 6 shows this effect.

Literature shows that the cooling rate plays an important role in the refinement of metal structures. A high mold temperature allows a low cooling rate. On the other hand, increasing the initial mold temperature could be related to the increase of the solidification time. This later decreases when the temperature of the preheating of the mold changes from 300°C to 150°C. Indeed, the solidification time increases from 277 s to 379 s for untreated samples. It value raises from 228 s to 315 s for the grain refined samples. This experimental finding is corroborated by [11].

High cooling rate and short solidification time refines the structure of the casting and increases grain density. This is in accordance with LY. Zhang and K.L. Davami [30,31] findings for A356. Moreover, the observed shift in the solidification time might be affected by the elevated concentration of α-Al in the liquid prior to the eutectic nucleation.

It is noted that the effect of grain refinement on the SDAS under the conditions where the mold was preheated to 150°C is more striking. The highest liquidus temperature was observed for cast samples after refinement in the preheated mold at 300°C. This is in contrast to the fact that the lowest values of SDAS were found for the case where the refined metal was cast in a preheated mold to 150°C. The results of this study show that changes in liquidus temperature can be correlated with the microstructure obtained, but it does not take into account the mold temperature variation.

When the mold temperature shift up from 150 to 300°C, the eutectic time increases from 119 s to 192s for the untreated samples and from 118 s to 152.5 s for the grain-refined samples poured. In the case of the mold preheated at 300°C we noticed that the eutectic time decreases significantly without a change in the eutectic temperature for the grain-refined samples. This indicates a rapid solidification of the Al-Si eutectic phase. From these data, we can affirm that the eutectic time is affected by the grain refiner addition.

When the SDAS is small, eutectic formation speed increases. Therefore, the dendrite matrix formation affects eutectic solidification. If we recognize that the eutectic formation speed is affected by the grain refinement, one can not affirm that it has any effect on eutectic phase morphology (acicular).

4. Conclusion

In the present work, the study of AlSi9 cast alloy has been undertaken. The grain size refiner addition is a practical solution to obtain refined microstructure. The effects of Titanium refinement and initial mold temperature on the microstructure of the alloy AlSi9 have been studied. Grain refinement efficiency was assessed by microstructural and thermal analyses.

The experimental results revealed that the grain size refiner changes the cells morphology from a columnar dendritic to a multiple spherical cells. The solidification parameters are affected by Titanium grain refinement. In-situ thermal analysis technique is of great practice for foundry man to estimate the refinement degree of Al-Si alloys. The solidification time and specially the eutectic phase formation time have decreased by addition of grain size refiner. Moreover, the decrease in solidification time brought about by mold temperature variation has an effect more pronounced when grain refiner is added. These changes do not affect the eutectic phase morphology and the eutectic temperature. The industrials can use the cooling rate variation to enhance the grain refiner effect.

REFERENCES

[1] S. Pietrowski, C. Rapiejko, Arch. Foundry Eng. **11** (3), 177-186 (2011).

[2] Y.M. Li, R.D. Li, Sci. Technol. Adv. Mater. **2** (1), 277-280 (2001).

[3] L.A. Dobrzanski, M. Krupinski, B. Krupinska, J. Achiev. Mater. Manuf. Eng. **27**, 23-26 (2008).

[4] B.P. Reis, R.P. França, J.A. Spim, J. Alloys Compd. **549**, 324-335 (2013).

[5] L. Ceschini, A. Morri, A. Morri, A. Gamberini, Mater. Des. **30**, 4525-4531 (2009).

[6] D.G. Mallapur, K.Rajendra Udupa, S.A. Kori, Int. J. Eng. Sci. Technol. **2** (9), 4487-4493 (2010).

[7] J. Wang, S. He, B. Sun, J. Mater. Sci. Technol. **141**, 29-34 (2003).

[8] J. Wang, S. He, B. Sun, K. Li, Mater. Sci. Eng. A **338** (1-2), 101-107 (2002).

[9] P. Li, V.I. Nikitin, E.G. KAndalova, K.V. Nikitin, Mater. Sci. Eng. **332** (1-2), 371-374 (2002).

[10] X. Hu, F. AI, H. Yan, Acta Metallurgica Sinica **25** (4), 272-278 (2012).

[11] M. Easton, D. StJohn, Metall. Mater. Trans. A **30** (6), 1613-1623 (1999).

[12] M. Easton, D. StJohn, Metall. Mater. Trans. A **30A**, 1625-1633 (1999).

[13] T.E. Queted, A.L. Greer, Acta Materialia **53**, 4643-4653 (2005).

[14] S. Seifeddine, T. Sjogren, I. Svensson, Metall. Sci. Technol. **25** (1), 12-22 (2007).

[15] L.A. Dobrzanski, R. Maniara, J.H. Sokolowki, Arch. Mater. Sci. Eng. **28** (2), 105-112 (2007).

[16] D. Casari, M. Merlin, G.L. Garagnani, Metall. Sci. Technol. **31** (1), 24-34 (2013).

[17] S.G. Shabestari, M. Malekan, J. Alloys Compd. **492** (1-2), 134-142 (2010).

[18] A.A. Canales, J. Talamantes-Silva, D. Gloria, S. Valtierra, Thermochim Acta **510** (1-2) 82-87 (2010).

[19] V.A. Hosseini, S.G. Shabestari, R. Gholizadeh, Mater. Des. **50**, 7-14 (2013).

[20] M. Krupinski, K. Labisz, L.A. Dobrzanski, J. Achiev. Mater. Manuf. Eng. **38** (2), 115-122 (2010).

[21] A. Hamadellah, A. Bouayad, C. Gerometta, J. Mater. Process. Technol. **244**, 282-288 (2017), DOI: 244. 10.1016/j.jmatprotec.2017.01.030.

[22] J. Pavlović-Krstić, R. Bähr, G. Krstić, Metall. Mater. Eng. **15** (2), 106-113 (2009).

[23] Q.G. Wang, M. Praud, A. Needleman, K.S. Kim, Acta Mater. **58** (8), 3006-3013 (2010).

[24] M. Brůna, A. Sládek, L. Kucharčík, Arch. Foundry Eng. 12, 5-8 (2012).

[25] B. Ait El Haj, A. Bouayad, M. Alami, Int. Lett. Chem. Phys. Astron. **55**, 12-18 (2015).

[26] E. Vandersluis, C. Ravindran, Metallogr. Microstruct. Anal. **6**, 89-94 (2017).

[27] M.A. Easton, D.H. StJohn, Mater. Sci. Eng. A **486** (1-2), 8-13 (2008).

[28] A. Niklas, U. Abaunza, A.I. Fernández-Calvo, J. Lacaze, China Foundry **8**, 89-95 (2011).

[29] M. Malekan, D. Dayani, A. Mir, J. Therm. Anal. Calorim. **115**, 393 (2014).

[30] L.Y. Zhang, Y.H. Jiang, Z. Ma, S.F. Shan, Y.Z. Jia, C.Z. Fan, W.K. Wang, J. Mater. Process. Technol. **207** (1-3), 107-111 (2008).

[31] K. Davami, M.K. Besharaty, in 8th WSEAS Int. Conf. on Robotics, Control And Manufacturing Technology, Hangzhou 127-137 (2008).